

# A numerically efficient approach to the modelling of double-Qdot channels

## Abstract

We consider the electronic properties of a system consisting of two quantum dots in physical proximity, which we will refer to as the double-Qdot. Double-Qdots are attractive in light of their potential application to spin-based quantum computing and other electronic applications, e.g. as specialized sensors. Our main goal is to derive the essential properties of the double-Qdot from a model that is rigorous yet numerically tractable, and largely circumvents the complexities of an *ab initio* simulation. To this end we propose a novel Hamiltonian that captures the dynamics of a bi-partite quantum system, wherein the interaction is described via a Wiener-Hopf type operator. We subsequently describe the density of states function and derive the electronic properties of the underlying system. The analysis seems to capture a plethora of electronic profiles, and reveals the versatility of the proposed framework for double-Qdot channel modelling.

## Keywords

Qdot • double-Qdot channel • composite quantum system • nanoelectronics

PACS: 68.65.Hb, 73.63.Kv, 85.35.Be, 02.10.Yn

MSC: 81Q10, 81Q15, 81Q37, 82D37, 82D80, 94C99

© 2013 A. Shamloo et al., licensee Versita Sp. z o. o. This work is licensed under the Creative Commons Attribution-NonCommercial-NoDerivs license (<http://creativecommons.org/licenses/by-nc-nd/3.0/>), which means that the text may be used for non-commercial purposes, provided credit is given to the author.

A. Shamloo\*, A.P. Sowa

*Department of Mathematics and Statistics,  
University of Saskatchewan  
106 Wiggins Road, Saskatoon, SK S7N 5E6, Canada*

Received 7 June 2013

Revised 31 July 2013

Accepted in revised form 5 August 2013

## 1. Introduction

In the last decade the theory and modelling of quantum dots have attracted a lot of attention and, indeed, the topic may be regarded as one of the central ones in the area of nanotechnology. Researchers have been successful in applying the *ab-initio* DFT simulation to explain the fundamental characteristics of a single quantum dot, which is typically considered as an artificial molecule, see e.g. [12, 13]. More recently there has been a lot of enthusiasm about nano-systems that consist of a pair of interacting quantum dots, here referred to as the double-Qdots. One of the remarkable examples is a double-Qdot comprising two *single-electron* quantum dots, see [15] and also [5]. Since these double-Qdots provide a means for controlling the electron spin via gate potentials—effectively implementing a spin-swap which is a fundamental quantum computing operation, [11]—they may well become the enabling hardware components of a quantum computer. Some very significant progress toward developing addressable quantum registers based on this type of technology was reported in [3]. A very promising feature of these new structures is their comparatively long coherence time. Of course, apart from quantum computing, the double-Qdots are bound to find other electronic applications, e.g. substituting for the traditional piezoelectric sensors, [9].

In light of this it is vital to develop good models for the electronic structure of double-Qdot systems and, indeed, the topic attracts a lot of attention. Of note are the early *ab initio* models, [16] or [20]. In addition, there has been progress

\* E-mail: [arash.shamloo@usask.ca](mailto:arash.shamloo@usask.ca) (Corresponding author)

in the modelling of a double-Qdot with metal contacts via the Non-equilibrium Green's Function Theory (NEGF). In particular, in [11] the authors assessed the validity of the equation of motion approach to the NEGF formalism specifically for a double-Qdot coupled with two contacts. The model takes into account both intra- and inter-dot Coulomb interactions. In general, the equation of motion NEGF formalism provides a qualitative description of transport phenomena that occur in strongly correlated systems, such as the Coulomb blockade effect and the Kondo effect. The authors study the effect of different approximate closures to the equation of motion NEGF formalism on steady state properties within an extended Hubbard model (also known as the double Anderson model). For comparison in [18] the authors consider a NEGF model based on a Hubbard type Hamiltonian, which accounts for tunneling type electron transfer between the two Qdots as well as the isolator-type electrostatic Coulomb interaction between them. The effect of contacts is also modelled via a tunneling electron transport. Yet another approach is taken in [6] wherein the electron transport, in structures such as the Qdots or single molecules, is captured via a quantum master equation. Naturally, this is meant as a brief introductory outline. While a complete literature review would go beyond the scope of this article, we return to the topic of NEGF and consider some additional aspects of this theory in Section 7.

It is vital to realize that a typical model of a double-Qdot system, be it of the *ab initio* or the NEGF type requires intensive computation. At the same time some applications of modelling—such as, say, production quality control, but also numerical experimentation for the sake of fundamental research—require high numerical efficiency ensuring real time computability. In this article we undertake to consider a new class of models for double-Qdots, which enable some scalability of computational complexity. The proposed composite-quantum-system type model is to our best knowledge conceptually novel and hitherto unexplored. It is based on a Hamiltonian for a bipartite quantum system, wherein the subsystem Hamiltonians are given *a priori*, and the interaction term is constructed with the use of a Wiener-Hopf type operator, see e.g. [1, 10]. Our decision to focus on this type of interaction term arose from a dictum that if a new mathematical structure is to be constructed to capture the essence of an element of increased complexity, it is probably best done with as much conceptual parsimony and as few additional “ingredients” as possible. Indeed, the proposed model is perhaps the simplest possible, given that it must incorporate each single Qdot’s dynamics and needs to account for the Qdot-Qdot interaction. We emphasize that the interaction is modelled at a rather general level to avoid the complexity trap that would be inevitable in an *ab initio* approach. The type of construction being proposed is perhaps somewhat reminiscent of the classical Jaynes-Cummings model, [7, 17], frequently evoked in Quantum Optics. However, in stark contrast to the Jaynes-Cummings Hamiltonian our model incorporates a high-dimensional parameter (the kernel function) which, by design, can be fitted to a physical system *a posteriori*.

One of the main goals of this work is to examine the cumulative density of states function,  $N(E)$ , arising from the proposed Hamiltonian. We have conducted extensive numerical simulations to understand the dependence of  $N(E)$  on the choice of the underlying parameters. As it turns out, the choice of parameters, especially the kernel function, strongly affects the characteristics of  $N(E)$ , which bodes well for the model’s applicability and versatility. We apply the results concerning  $N(E)$  to draw conclusions about the electronic characteristics of the double Qdot channel. One of our main findings is summarized in Fig. 4. Our model suggests that the functional features of such systems should fall within several distinct categories. In Section 6 we give a brief qualitative comparison of these predictions to the known experimental data. In Section 7 we discuss a range of issues pertaining to the numerical efficiency of the model at hand.

## 2. Constructing the composite system Hamiltonian

We wish to consider a quantum system that consists of two distinguishable components (subsystems), e.g. two distinct Qdots. We assume that the subsystem properties are well understood and given to us *a priori* as constituents of the model. More specifically, let the dynamic properties of these components, when in isolation, be captured by Hamiltonians  $H_i : \mathcal{H}_i \rightarrow \mathcal{H}_i$  ( $i = 1, 2$ ), both having pure-point spectrum. In order to fix notation let us specify the eigenstates:

$$H_1(\psi_k) = E_k \psi_k, \quad \text{and} \quad H_2(\phi_l) = F_l \phi_l,$$

where, for convenience, we allow the eigenstates to be indexed by arbitrary integers, i.e.  $k, l \in \mathbb{Z}$ . Note that the two bases — i.e.  $\{\psi_k\}_{k \in \mathbb{Z}}$  and  $\{\phi_l\}_{l \in \mathbb{Z}}$  — furnish the Hilbert space isomorphisms  $\mathcal{H}_i \cong l_2(\mathbb{Z})$  ( $i = 1, 2$ ).

Next, construct the composite system Hamiltonian  $H : \mathcal{H}_1 \otimes \mathcal{H}_2 \rightarrow \mathcal{H}_1 \otimes \mathcal{H}_2$  in the form

$$H = H_1 \otimes I + I \otimes H_2 + \lambda H_{int}, \tag{1}$$

which accounts for inter-component interaction. We wish to propose a simple model for  $H_{int}$ . First, observe that the basis  $\{\psi_k \otimes \phi_l\}_{(k,l) \in \mathbb{Z}^2}$  furnishes an identification  $\mathcal{H}_1 \otimes \mathcal{H}_2 \cong l_2(\mathbb{Z}) \otimes l_2(\mathbb{Z}) \cong l_2(\mathbb{Z}^2)$  via a unitary map  $T$ :

$$T : \mathcal{H}_1 \otimes \mathcal{H}_2 \longrightarrow l_2(\mathbb{Z}^2)$$

$$T : |\psi_k\rangle|\phi_l\rangle \longmapsto \delta_{(k,l)}.$$

In other words, for a composite system state vector  $\Psi \in \mathcal{H}_1 \otimes \mathcal{H}_2$  we obtain  $T\Psi = X \in l_2(\mathbb{Z}^2)$ , such that

$$\Psi = \sum_{(k,l) \in \mathbb{Z}^2} X(k,l) |\psi_k\rangle|\phi_l\rangle \quad (\text{notation: } |\psi_k\rangle|\phi_l\rangle = \psi_k \otimes \phi_l). \quad (2)$$

Second, consider a matrix  $K \in l_2(\mathbb{Z}^2)$  (whose properties will be specified later). We attempt to prescribe the interaction Hamiltonian by

$$H_{int}\Psi = \sum_{(k,l) \in \mathbb{Z}^2} Y(k,l) |\psi_k\rangle|\phi_l\rangle,$$

where

$$Y = K * X, \quad \text{i.e.} \quad Y(n_1, n_2) = \sum_{(k,l) \in \mathbb{Z}^2} K(n_1 - k, n_2 - l) X(k, l).$$

In other words,

$$H_{int}\Psi = T^*K * T\Psi \quad \text{equivalently} \quad TH_{int}T^* = K *. \quad (3)$$

Of course, we need to specify conditions on  $K$  for  $H_{int}$  to be a viable interaction Hamiltonian. The first issue of concern is ensuring self-adjointness  $H_{int}^* = H_{int}$ . In order to resolve the problem we proceed as follows. Let us define a unitary operator

$$\mathcal{U} : \mathcal{H}_1 \otimes \mathcal{H}_2 \longrightarrow L_2([0, 2\pi]^2)$$

$$|\psi_k\rangle|\phi_l\rangle \longmapsto e^{ikx} e^{ily},$$

and let  $\mathcal{F}$  denote the unitary map of the Fourier transform, i.e.

$$\mathcal{F} : L_2([0, 2\pi]^2) \longrightarrow l_2(\mathbb{Z}^2),$$

$$e^{ikx} e^{ily} \longmapsto \delta_{(k,l)}.$$

We write  $\mathcal{F}X = \check{X}$ . As is well known the Fourier transform is an algebra homomorphism which trades multiplication for convolution. Therefore,  $K * X = \mathcal{F}(\check{K} \cdot \check{X})$ . Let  $V = \check{K} \in L_2([0, 2\pi]^2)$ , and let  $V_\times : L_2([0, 2\pi]^2) \rightarrow L_2([0, 2\pi]^2)$  denote the operator of multiplication by  $V$ . By (3) we have  $TH_{int}T^* = \mathcal{F}V_\times\mathcal{F}^*$  or, equivalently,

$$H_{int} = T^*\mathcal{F}V_\times\mathcal{F}^*T = \mathcal{U}^*V_\times\mathcal{U}. \quad (4)$$

It is now clear that  $H_{int}$  is formally self-adjoint iff  $V = \check{K}$  is real valued. This observation is also helpful in describing the analytic properties of  $H_{int}$ , although we do not undertake to do so in this article, which is focused on numerical experimentation.

### Remark 1.

In the special case of  $H_1 = \frac{d^2}{dx^2}$ ,  $H_2 = \frac{d^2}{dy^2}$ , with  $(x, y)$  in the flat torus, the unitary operator  $\mathcal{U}$  in (4) is in fact an identity, and so  $H$  given by (1) is in fact equivalent to the Schrödinger operator with the Coulomb potential  $V = \check{K} \in L_2([0, 2\pi]^2)$ . In light of this (1) may be viewed as a generalization of the standard Schrödinger model.

### 3. Examining the special case

For the convolution kernel  $K = \delta_{(1,-1)} + \delta_{(-1,1)}$ , one obtains

$$H_{int}|\varphi_k\rangle|\psi_l\rangle = |\varphi_{k-1}\rangle|\psi_{l+1}\rangle + |\varphi_{k+1}\rangle|\psi_{l-1}\rangle.$$

Furthermore, let us fix the subsystem Hamiltonians  $H_1, H_2$  with equal discrete energy spectra  $E_n = F_n$ . We are going to represent the composite system Hamiltonian in the basis  $\{|\varphi_k\rangle|\psi_l\rangle\}$  ordered in a special way as follows:

$$\begin{aligned} &|\varphi_0\rangle|\psi_0\rangle, && (k+l=0) \\ &|\varphi_1\rangle|\psi_0\rangle, |\varphi_0\rangle|\psi_1\rangle, && (k+l=1) \\ &|\varphi_2\rangle|\psi_0\rangle, |\varphi_1\rangle|\psi_1\rangle, |\varphi_0\rangle|\psi_2\rangle, && (k+l=2) \\ &|\varphi_3\rangle|\psi_0\rangle, |\varphi_2\rangle|\psi_1\rangle, |\varphi_1\rangle|\psi_2\rangle, |\varphi_0\rangle|\psi_3\rangle, && (k+l=3) \\ &\vdots && \end{aligned}$$

Observe

$$\begin{aligned} H|\varphi_2\rangle|\psi_0\rangle &= (E_2 + E_0)|\varphi_2\rangle|\psi_0\rangle + \lambda|\varphi_1\rangle|\psi_1\rangle, \\ H|\varphi_1\rangle|\psi_1\rangle &= (E_1 + E_1)|\varphi_1\rangle|\psi_1\rangle + \lambda|\varphi_0\rangle|\psi_2\rangle + \lambda|\varphi_2\rangle|\psi_0\rangle, \\ H|\varphi_0\rangle|\psi_2\rangle &= (E_0 + E_2)|\varphi_0\rangle|\psi_2\rangle + \lambda|\varphi_1\rangle|\psi_1\rangle, \dots \text{ etc.} \end{aligned}$$

Thus  $H$  is represented by the following block structured matrix:

$$H = \begin{pmatrix} E_0 + E_0 & 0 & 0 & 0 & 0 & 0 & \dots & \dots \\ 0 & E_1 + E_0 & \lambda & 0 & 0 & 0 & \dots & \dots \\ 0 & \lambda & E_0 + E_1 & 0 & 0 & 0 & \dots & \dots \\ 0 & 0 & 0 & E_2 + E_0 & \lambda & 0 & \dots & \dots \\ 0 & 0 & 0 & \lambda & E_1 + E_1 & \lambda & \dots & \dots \\ 0 & 0 & 0 & 0 & \lambda & E_0 + E_2 & \dots & \dots \\ \vdots & \vdots & \vdots & \vdots & \vdots & \vdots & \ddots & \vdots \end{pmatrix}$$

When the energy levels are those of a harmonic oscillator<sup>1</sup>, i.e.  $E_n = \frac{2n+1}{2}$ , the  $H$  matrix consists of increasing diagonal blocks of the form:

$$H_N = \begin{pmatrix} N & \lambda & 0 & \dots & 0 & 0 \\ \lambda & N & \lambda & \dots & 0 & 0 \\ 0 & \lambda & N & \dots & 0 & 0 \\ \vdots & \vdots & \vdots & \ddots & 0 & 0 \\ 0 & 0 & 0 & \dots & N & \lambda \\ 0 & 0 & 0 & \dots & \lambda & N \end{pmatrix}$$

The eigenvalues of such matrices may be calculated explicitly, [2], by using the row expansion of the determinant that results in a recurrence relation. Namely, the eigenvalues turn out to be:

$$E_{N,k} = N - 2\lambda \cos \frac{k\pi}{N+1}, \quad k = 1, \dots, N. \tag{5}$$

The doubly-indexed collection  $\{E_{N,k} : k = 1, \dots, N, N = 1, 2, 3, \dots\}$  is the complete set of the eigenvalues of the  $H$  matrix.

<sup>1</sup> Since the model is parametric by design and all the essential predictions are of qualitative nature, the physical constants may be viewed as parameters and are here set at trivial values for convenience.

We have used the above observation to test the correctness as well as the accuracy of the general numerical experiments with the Hamiltonian (1)–(3). In order to briefly summarize our findings, let  $\{e_i : i = 1, 2, 3, \dots, N(N+1)/2\}$  be the complete set of *theoretical* eigenvalues of  $H$ , i.e. the eigenvalues are determined via formula (5) and ordered according to their magnitudes. Similarly, let  $\{\mathcal{E}_i : i = 1, 2, 3, \dots, N(N+1)/2\}$  denote the magnitude-ordered eigenvalues of  $H$  resulting from *numerical simulation*. The maximal distance  $|e_i - \mathcal{E}_i|$  may then be regarded as a measure of accuracy of the numerical schema used to obtain  $\{\mathcal{E}_i\}$ . In this way we have established convincing evidence for the reliability of our specific numerical schema, which is described in the Appendix. To give an example, we find that for  $N = 21$  and  $\lambda = 1$  or  $\lambda = 10$ ,  $\max\{|e_i - \mathcal{E}_i| : i = 1, 2, 3, \dots, N(N+1)/2\} \cong 10^{-14}$  and for  $\lambda = 100$  the accuracy is hardly diminished at  $10^{-13}$ .

#### 4. Modelling a double-Qdot channel

We wish to consider a conceptual semiconductor channel device comprising two (similar or identical) quantum dots suspended in between metal contacts (source and drain), see Fig. 1. In a laboratory setting the Qdots become coupled when brought into physical proximity, close enough for the electron clouds to interleave. It is intuitively natural to expect that within a moderate range of the inter-Qdot distances the qualitative nature of the interaction remains unchanged, while its strength should depend on the actual distance, e.g. it might be in the inverse proportion to it. Note that the difference between a nanoscopic system such as the one at hand and a microscopic one is that it precludes the possibility of chemical bonding. We believe that systems as these may find numerous applications in electronics and sensing, including the problem of detecting and quantifying the strength of micro-vibrations. In light of this, we find it interesting to understand the dependence of their *strength of interaction-to-conductivity* characteristic on the parameters characterizing a given set of components and their geometry. This is the focus of the remainder of this article.

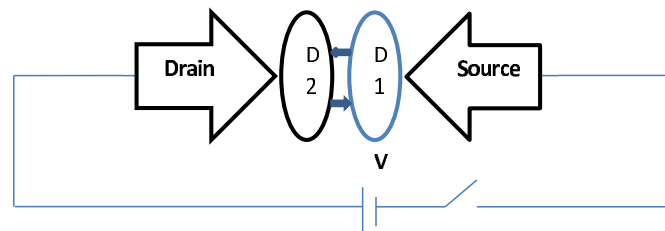


**Fig 1.** The simplest circuit with the double Qdot channel (DQDC).

In order to come up with a workable conceptual model of the system at hand, we will ignore the effect of the contact-Qdot interaction (— for additional comments see Remarks at the end of this section), and focus solely on the double Qdot subsystem. Subsequently, we elect to view the double Qdot as a bipartite quantum system, and construct its model via Hamiltonians of type (1)–(3), experimenting with different choices of the constituent parameters, including several deliberate modifications of the kernel function  $K$ . The role of the kernel is to capture, at least qualitatively, the inter-Qdot interaction, while the parameter  $\lambda$  moderates its strength. In light of the proposed interpretation  $\lambda$  may be conceived of as a parameter quantifying the effect of the adjustment of the inter-Qdot distance.

Another external parameter is the number of electrons, which we fix throughout the discussion, assuming that each of the Qdots has  $2N$  orbital electrons. Furthermore, we ignore the effect of temperature, e.g. when the Qdots are in isolation, the electrons occupy the first  $N$  of the energy levels determined by  $H_1$  and  $H_2$  respectively, i.e. two opposite spin electrons per level. For simplicity, we assume that  $H_1 = H_2$  are the harmonic oscillators.

At equilibrium, the system has a common Fermi energy  $E_F$  which is equal to the electrochemical potentials of source  $\mu_s$  and drain  $\mu_d$ . On the other hand, when voltage  $V$  is applied across the double-Qdot channel, the two electrochemical potential levels split ( $\mu_s - \mu_d = qV$ ). If  $\mu_s > E_F \geq \mu_d$ , with  $\mu_s$  sufficiently high, there exist unoccupied levels of energy in the molecule within the range  $[\mu_d, \mu_s]$ . In these conditions a current is forced through the double Qdot channel, see the schematic representation in Fig. 2. The electric charge is transported in charge quanta of  $-1e$  by electrons.

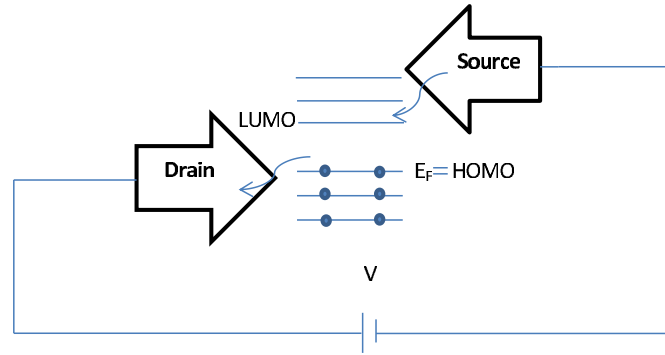


**Fig 2.** Schematic representation of the concepts used to determine the conductivity of the DQDC. Note that the Fermi energy  $E_F$  exactly coincides with the HOMO level (at zero temperature).

We discuss the problem of calculating the conductivity of a double Qdot channel placed between the source and drain contacts (DQDC for short). To this end, we invoke *the density of states* function  $D(E)$ , and the *cumulative density of states* function  $N(E)$ . Denoting  $\mathcal{E}_i$  the eigenvalues of the composite system Hamiltonian  $H$ , we have

$$D(E) = \sum_i \delta(E - \mathcal{E}_i),$$

and

$$N(E) = \int_{-\infty}^E D(E)dE.$$

Briefly, since  $D(E)$  is a string of delta functions,  $N(E)$  is the counting function, like a staircase function, which jumps up by one as the variable  $E$  passes through each energy level.

As mentioned above, the first assumption is that the DQDC is a quantum system whose dynamics is governed by the Hamiltonian  $H$  of the type (1)-(3). Secondly, we assume that the conductivity  $\kappa(E)$  of the DQDC per spectral range  $dE$  is proportional to the number of energy levels in  $[E, E + dE]$ . More precisely, we have  $\kappa(E) = kD(E)$ , where the coefficient of proportionality  $k$  depends on a variety of external parameters such as the effective electron mass, the mean free time, and the geometry of the system, [4]. Thus, assuming for simplicity  $\mu_d = 0$ ,  $\mu_s = qV$ , the overall conductivity is the sum of  $\kappa(E)$  over the span of unoccupied energy levels below the applied potential:

$$\kappa = \int_{E_F}^V \kappa(E) dE = k[N(V) - N(E_F)]. \tag{6}$$

This formula is the foundation for the numerical study of the conductivity properties of a DQDC in the next section.

**Remark 2.**

In applications a DQDC element is typically hooked up to a circuit via a pair of contacts (metal leads). While the discussion of DQDC carried out above abstracts from the effects induced by the contacts, the conductivity of the device as a whole could still be modelled via an effective Hamiltonian. However, in some applications it is of interest to separate the effect of contacts and make it an inherent part of the model. As mentioned in the Introduction such effects are typically modelled within the framework of the NEGF (also known as the Keldysh calculus)<sup>2</sup>. Following [14] we observe that at the phenomenological level the main effect of coupling to the contacts is *energy level broadening* as well as a *shift of the effective Fermi energy level*. The energy level broadening induces flow of a fractional-charge

<sup>2</sup> A similar approach was taken early on in a study of the conductivity of a molecule suspended between two metal leads, [14].

current through the DQDC, even if there are effectively no “pure energy levels” in the interval  $[\mu_d, \mu_s]$ . Also, the Fermi energy level is effectively shifted to occupy a position mediating between HOMO and LUMO, whose exact value is typically left free as an adjustable parameter that may be fitted to a system *a posteriori*. (Note that if charge transport is effected in integer quanta, the Fermi energy coincides with the HOMO level, as schematically indicated in Fig. 2.) A slew of additional corrections would originate from lifting the assumption of absolute-zero temperature (leading to a different statistics of energy-level occupation). At the end of Section 7 we briefly discuss the consequences for numerical efficiency that stem from extending the model to explicitly account for the coupling to contacts.

## 5. Numerical Experiments

We report the results of a numerical study of the  $\lambda$ -to- $\kappa$  characteristic of a DQDC with different choices of the kernel function  $K$ . Recall that we base the model of a DQDC on a Hamiltonian of type (1)–(3), and calculate the across-channel conductivity via formula (6). Another of the underlying *a priori* assumptions is the number of occupied levels, i.e. the number of orbital electrons. We have developed numerical algorithms in the MATLAB environment. At this stage, the real-time experimentation is feasible only for relatively small numbers of orbital electrons. Nevertheless, we believe these results outline a qualitatively adequate picture. Our main findings are presented in Figs. 3. The graphs illustrate the dependence of  $N(E)$  on  $K$ . We have used the following two kernel types:

1. The “special”  $K$  is as in Section 3.
2. The “periodic”  $K$  is a kernel matrix built in two steps: First, take a matrix  $L$  whose rows are filled with the values of a discretized periodic function, e.g.  $\sin$ . Second, take  $K$  to be the Fourier transformed  $L$ .

It is interesting to observe that regardless of the kernel the graphs tend to be characterized by stronger concavity of their course scale shape for smaller values of  $\lambda$ .

Fig. 4 displays the dependence of DQDC’s conductivity  $\kappa$  on the coupling constant  $\lambda$  for three different  $K$ s. In addition to the two kernel types described above, we have also considered a random type kernel, i.e. a kernel obtained via the discrete Fourier transform of a random matrix<sup>3</sup>. Clearly the three  $\lambda$ -to- $\kappa$  curves display individualized and significantly differentiated characteristics, which evidences the proposed model’s versatility. We predict all the three  $\lambda$ -to- $\kappa$  profiles and possibly more to be physically realizable. We also expect the model to be broadly adaptable to the analysis of other systems with bi-partite architectures.

*Remark.* An additional, finer characterization of the properties of the model at hand depends on the statistical profile of the fine-scale oscillations found in the  $N(E)$  curves (—see box inserts in Figs. 3). We anticipate further results in this direction which will be reported in future articles.

## 6. Qualitative comparison to the experimental data

Several experimental studies of the DQDC type structures may be found in the literature, e.g. [8]. In particular, the aforementioned article [3] reports, among other results, conductivity measurements of a particular DQDC structure, referred to as the single electron transistor (SET). The electronic characteristic of a SET is controlled by a pair of gate potentials  $(V_{G1}, V_{G2})$ . Clearly, the gate potentials adjust the electrochemical potentials of the two QDots. However, their overall influence on the structure and function of a SET is more complex than that as even the fundamental Hamiltonian is profoundly affected by these parameters. Indeed, the external electric field modifies the shape of the electronic wave function and through that influences Coulomb interactions as well as the hyperfine coupling between the electron and nuclear spins. The reported measurement of source-drain current at a constant applied source-drain bias, see Fig. 1f–g therein, demonstrates strong dependence of conductivity on  $(V_{G1}, V_{G2})$ . One of the striking features is the presence of abrupt, nearly discontinuous, changes in conductivity as  $(V_{G1}, V_{G2})$  traverses different regions of the plane. This particular result may be reinterpreted within the framework proposed here. Indeed, we postulate that the two-dimensional  $(V_{G1}, V_{G2})$ -space can be mapped into our model’s high-dimensional  $(\lambda, K)$ -space in such way as to carry over the essential features of the effective Hamiltonian. Note that due to inherent complexity the exact dependence of the

<sup>3</sup> Here, a random matrix means a matrix populated by uniformly distributed (in  $[0, 1]$ ) random numbers obtained with one of the MATLAB’s standard random number generators.

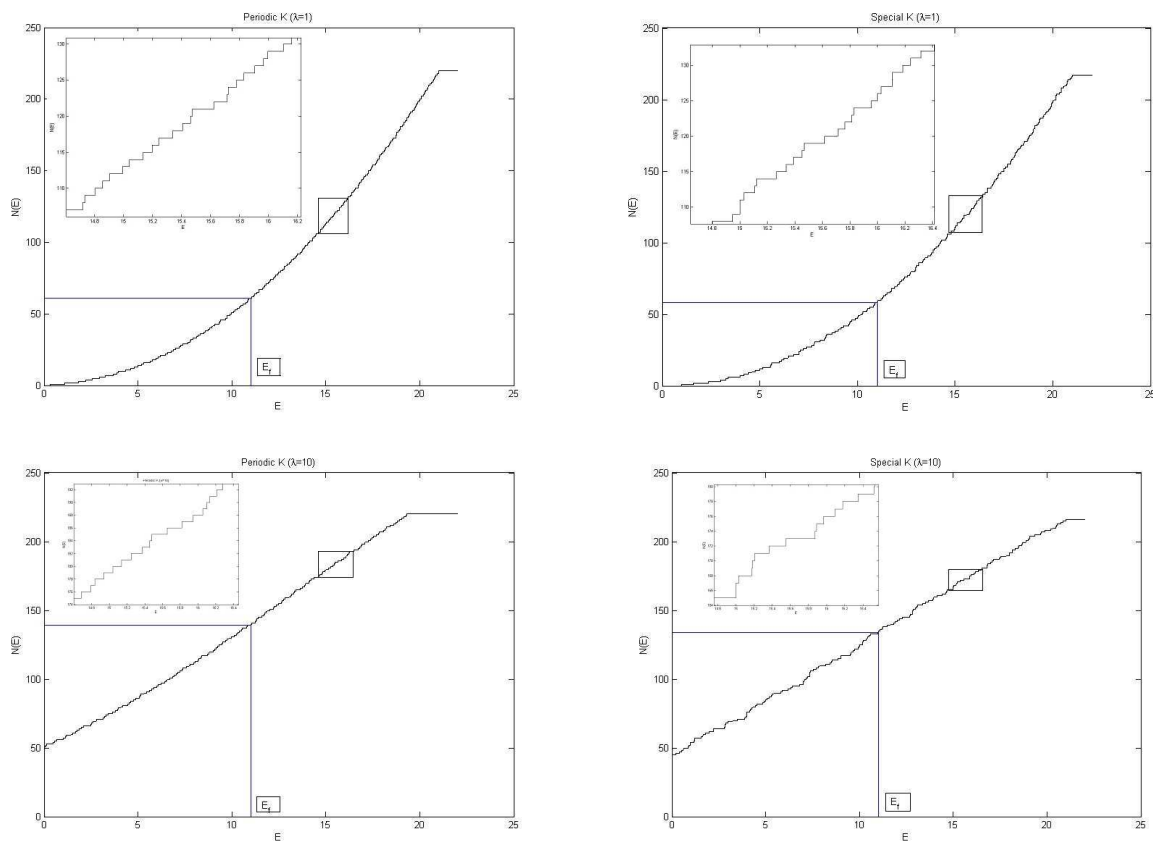


**Fig 3.** The cumulative density of states function  $N(E)$  for the periodic and “special” kernels  $K$  at two different values of the coupling constant  $\lambda$ .

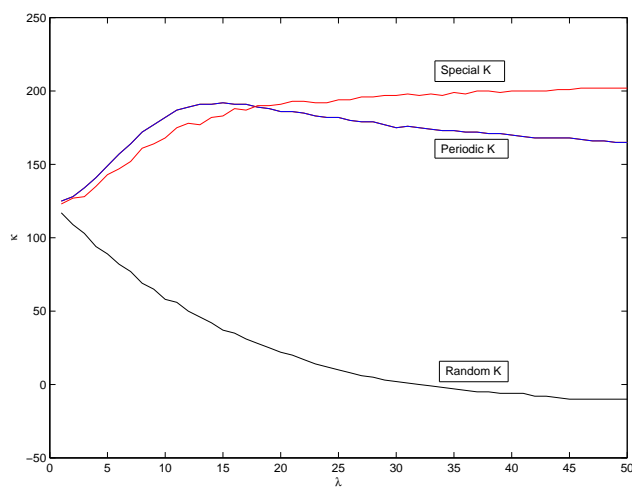


**Fig 4.** Conductivity  $\kappa$  of a double-Qdot channel (DQDC) as a function of the coupling constant  $\lambda$  for three different kernel functions. For computational efficiency the number of orbital electrons has been fixed at a low value (21).

Hamiltonian on the gate potentials is unknown. Nevertheless, there are strong similarities between our predictions and the reported experimental findings. Indeed, our simulations demonstrate that continuous change in  $\lambda$  effects continuous adjustment of the conductivity, whereas qualitative change in  $K$  effects conductivity jumps, Fig. 4. In light of that it should be possible, at least in principle, to find  $(\lambda, K) = \Phi[V_{G1}, V_{G2}]^4$  resulting in the accurate predicted conductivity function. Such a task might be attempted via the known techniques for automated parameter fitting.

## 7. A discussion of numerical efficiency

In some applications the speed of simulation is the most important parameter. When that is the case it is necessary for the modeller to have the option of easing the simulation accuracy for gains in computational time. This requirement seems to disadvantage simulation schemas based on *ab initio* models, or even higher-level models that rely upon geometrically localized description of the device in question. Indeed, in those cases the only possible speed gains come from relaxing the tolerance of parameter fitting rather than a reduction in the number of parameters itself. Therefore, when speed is of essence there arises a need for models that keep in check the number of tunable parameters, such as the one proposed here.

All simulation that is based on the *fundamental* (as contrasted with the merely *phenomenological*) principles unavoidably involves some computational constants: a computation of the eigenvalues of the matrix representing the Hamiltonian, parameter fitting via optimization algorithms, such as the genetic algorithm or the simulated annealing schema, etc. Given this constraint a speed-up may still be achieved by limiting the complexity of the Hamiltonian matrix. Such a feat may not always be possible, e.g. it is hard to reduce the complexity of a model that relies on the local geometric description of the simulated device. However, one may hope to achieve complexity reduction by delocalization of parameters, which is the approach we have taken.

Let us briefly compare the model proposed here with the one adopted in the highly regarded standard of nano-system simulation, specifically NEMO 3D,<sup>5</sup>. NEMO 3D is a remarkably versatile tool which enables simulation of nano-devices at a rather fundamental level. However, its demand for the computational power is indeed very high, and speed-up can only be achieved via parallel computation with an increased number of nodes. That computational rigidity is at least partly a by-product of the rigidity of the "bottom-up" models that NEMO 3D computation relies upon. Namely, NEMO 3D synthesizes a Hamiltonian of a nano-structure from a description of the global inter-atomic architecture as well as a relatively detailed description of localized atomic orbitals. In order to solve the model it is necessary to compute the eigenvalues of a large matrix whose characteristics are essentially beyond the modeller's control. In particular, this approach offers no possibility of building progressively less complex simplified models for a structure of interest.

In contrast, the model we propose does not incorporate any strictly geometric descriptions of the underlying physical structure. Thus far we observe sufficient flexibility within this framework to simulate fairly complex electronic spectra of structures such as the DQDC, and capture the essential features of their conductivity. Moreover, in the proposed approach there is a possibility of choosing the model complexity within the constraint of desired accuracy of its predictions. In particular, the Hamiltonians may have a block structure by design, offering easy parallelizability. This cannot be achieved with models that relate the Hamiltonian to the local geometric architecture of the device.

In our simulation schema, as in most other, the dominant factor determining the time of computation is the evaluation of the eigenvalues of the Hamiltonian matrix. A computation of the eigenvalues of an  $N \times N$  matrix requires  $O(N^3)$  arithmetical operations, and becomes prohibitively complex for large  $N$ . However, we note that in order to compute conductivity  $\kappa$ , defined in (5), only very selective information about the eigenvalues is used — namely, the number of eigenvalues in the interval  $[E_F, V]$ . Thus, for this application, the eigenvalues need not be known with high accuracy. Instead, it suffices to localize each eigenvalue inside or outside this interval. While further research is required to fully develop this idea, we expect an increased efficiency of such a computation can be obtained with suitable modifications of iterative schemas such as the celebrated Lanczos iteration, [19].

It is also interesting to briefly consider the changes that would result from extending our model to include an explicit discussion of contacts, particularly the effect it would have on the numerical complexity of the model. In essence

<sup>4</sup> Note that  $\Phi$  could turn out to be a nonlocal functional rather than just a local function.

<sup>5</sup> Introduction to the NEMO 3D Tool, <http://nanohub.org/resources/11080/download/>

the contacts are viewed as a quantum reservoir characterized by a Hamiltonian  $H_R$ . The NEGF type coupling of contacts to the central device is expressed via the super-system Hamiltonian

$$\tilde{H} = \begin{pmatrix} H & \tau \\ \tau^* & H_R \end{pmatrix},$$

where the interaction part  $\tau$  is typically a rectangular sparse matrix. The electronic conductivity through the core is then determined via the effective resolvent (alternatively called the Green's function)  $G = G(E)$ , which is defined via

$$(E - \tilde{H})^{-1} = \begin{pmatrix} G(E) & G_R(E) \\ G_R(E)^* & G_{RR}(E) \end{pmatrix},$$

While the sub-matrix  $G(E)$  is essential,  $G_R$  and  $G_{RR}$  are merely auxiliary in the construction and play no further role. It is easily seen that  $G(E) = [E - H - \Sigma]^{-1}$ , where  $\Sigma = \Sigma(E) = \tau[E - H_R]^{-1}\tau^*$ . The main observation of the NEGF theory is that the system's conductivity is determined by the quantity  $\text{Trace}[G \Gamma G^*]$  with  $\Gamma = \sqrt{-1} [\Sigma - \Sigma^*]$  in conjunction with the energy level occupation statistics. We observe that the NEGF framework is universal and can be developed for any core Hamiltonian  $H$ , including the Hamiltonians proposed here. However, most importantly, the resulting numerical schema involves the inversion of large matrices resulting in a substantially increased demand for the computational power.

## 8. Conclusion

We have analysed the electronic properties of a channel comprising two interacting quantum dots (DQDC) within the framework of a numerically efficient quantum model. The proposed model is based on a bipartite quantum system Hamiltonian with a novel Wiener-Hopf type interaction term. We have conducted a numerical analysis of the resulting cumulative density of states function and drawn conclusions regarding the dependence of the DQDC's conductivity on the coupling constant. Our results suggest that the proposed model is capable of capturing diverse DQDC characteristics. We consider the nano-structure at hand to be of interest because of its potential significance for next generation sensors and circuits.

## Acknowledgements

The authors are grateful to A. Zagoskin for suggesting helpful references. We are also indebted to the referees for a prudent review and a range of constructive questions and suggestions which helped us expand and improve this article. Finally, APS acknowledges the support of the Canadian Foundation for Innovation, grant LOF # 22117.

## APPENDIX—AN OUTLINE OF NUMERICAL ALGORITHMS

In order to ensure reproducibility of the reported results we outline the numerical procedures. The main task is to construct the composite system Hamiltonians of type (1)–(3). Let  $X$  denote an  $N \times N$  matrix representing the state of a composite system (—compare (2)). The preparatory phase consists of two parts: first, the construction of the interaction operator  $H_{int}$  which is a convolution type operator, roughly,  $H_{int}[X] = K * X$  and second, the construction of a non-interacting composite system Hamiltonian of the form  $\tilde{H} = H_1 \otimes I + I \otimes H_2$ . Note that the operators act on matrices, and hence the main challenge is in representing these operators in a suitable basis in the space of matrices. We describe this in more detail below.

The input data consist of:

- A  $p \times p$  matrix  $K$  (we take  $p$  odd for simplicity). Recall that for the final Hamiltonian to be a hermitian operator,  $\check{K}$  must have real entries.
- Two  $N$ -vectors  $h_1$  and  $h_2$ , each containing the ordered list of the eigenvalues of its corresponding subsystem Hamiltonian.
- A real number representing the coupling constant  $\lambda$ .

First, the interaction matrix  $H_{int}$  is built in steps as follows:

1. Choose a special basis in the space of  $N \times N$  matrices as follows:

$$X_{11}, (X_{12}, X_{21}), (X_{13}, X_{22}, X_{31}), \dots$$

(parentheses are only used to emphasize the pattern), where  $X_{ij}$  denotes a matrix with  $X_{ij}(i, j) = 1$  and zeros elsewhere.

2. Define  $C = conv2(K, X_{ij})$ . Subsequently, select the  $N \times N$  mid-centered sub-matrix of  $C$  and call it  $C_{ij}$ . (This is necessary because the numerical convolution algorithm results in an enlarged matrix which is inconsistent with the definition of  $H_{int}$ .)
3. Build an  $N^2$ -vector  $V_{ij}$  by reordering the entries of  $C_{ij}$  into a sequence, starting from the top right and proceeding through consecutive diagonals to the bottom left of  $C_{ij}$ . The following example illustrates the principle:

$$\text{If } C_{ij} = \begin{pmatrix} a_1 & a_2 & a_3 \\ b_1 & b_2 & b_3 \\ c_1 & c_2 & c_3 \end{pmatrix}, \text{ then } V_{ij} = [a_3, a_2, b_3, a_1, b_2, c_3, b_1, c_2, c_1]^T.$$

4. Build  $N^2 \times N^2$  matrix  $H_{int}$  whose columns are vectors  $V_{ij}$  ordered in the same way as the  $X_{ij}$  in step 1.

Second, one constructs the non-interacting part of the Hamiltonian, i.e.  $\tilde{H}$ :

1. Define  $H(i, j) = h_1(i) + h_2(j)$ .
2. Build an  $N^2$ -vector  $W$  by reordering the entries of  $H$  in a way analogous to step 3 above.
3. Define:  $\tilde{H} = \text{diag}(W)$  (a diagonal matrix with  $W$  filling the diagonal).

At this stage one is ready to define the total Hamiltonian:  $\text{Hamiltonian} = \tilde{H} + \lambda H_{int}$ . The Hamiltonian is now represented by a matrix, and one can rely on the MATLAB's standard 'eig' command to find its eigenvalues. Note that MATLAB utilizes the QR iteration algorithm to compute the eigenvalues of a matrix.

## References

- [1] B. Booss and D.D. Bleecker, *Topology and Analysis*. Springer, New York, (1985).
- [2] A. Bottcher and S.M. Grudsky, *Spectral Properties of Banded Toeplitz Matrices*. SIAM, (2005).
- [3] H. Buch, S. Mahapatara, R. Rahman, A. Morello, and M. Y. Simmons, Spin readout and addressability of phosphorus-donor cluster in silicon. *Nature communications*, (2013).
- [4] S. Datta, *Lessons from Nanoelectronics*. World Scientific, Singapore, (2012).
- [5] D. P. Divincenzo, Double quantum dot as a quantum bit. *Science*, **309**, 2173, (2005).
- [6] U. Harbola, M. Esposito, and S. Mukamel, Quantum master equation for electron transport through quantum dots and single molecules. *Phys. Rev B*, **74**, 235309, (2006).
- [7] E.T. Jaynes and F.W. Cummings, Comparison of quantum and semiclassical radiation theories with applications to the beam maser. *Proc. IEEE*, **59**(89), (1963).
- [8] T. Junno, S. B. Carlsson, H. Q. Xu, L. Samuelson, and A. O. Orlov, Single-electron tunneling effects in a metallic double dot device. *Applied Physics Letter*, **80**(4), 667–669, (2002).
- [9] K. Klantar-Zadeh and B. Fry, *Nanotechnology-Enabled Sensors*. Springer, New York, USA, (2008).
- [10] J.B Lawrie and I.D. Abrahams, A brief historical perspective of the wiener-hopf technique. *Engrg. Math*, **59**(4), 351–358, (2007).
- [11] T. J. Levy and E. Rabani, steady state conductance in a double quantum dot array: The nonequilibrium equation of motion green's function approach. *The Journal of Chemical Physics*, **138**, 164125, (2013).

- [12] E. Lipparini, *Modern many-particle physics*. World Scientific, Singapore, (2003).
- [13] J-L. Liu, Mathematical modeling of semiconductor quantum dots based on the nonparabolic effective-mass approximation. *Nanoscale Systems MMTA*, **1**(1), 58, (2012).
- [14] M. Paulsson, F. Zahid, and S. Datta, Electrical conduction through molecules. *Advanced Semiconductors and Organic Nano-Techniques*, (2003).
- [15] J. R. Petta, A. C. Johnson, J. M. Taylor, E. A. Laird, A. Yacoby, and M. D. Lukin et al., Coherent manipulation of coupled electron spin in semiconductor quantum dots. *Science*, **309**, 2180, (2005).
- [16] G. Shinkai, T. Hayashi, T. Ota, and T. Fujisawa, Correlated coherent oscillation in couple semiconductor charge qubit. *Superlattices and Microstructures*, **28**(4), (2000).
- [17] B. W. Shore and P. L. Knight, The Jaynes-Cummings model. *J. Mod. Opt.*, **40**, 1195, (1993).
- [18] D. Sztenkiel and R. Świrkowicz, Electron transport through quantum dot system with inter-dot coulomb interaction. *Acta Physica Polonica A*, **111**(3), 361–372, (2007).
- [19] L.N. Trefethen and M. Embree, *Spectra and Pseudospectra*. Princeton University Press, Princeton, New Jersey, (2005).
- [20] A.M. Zagoskin, *Quantum Engineering*. Cambridge University Press, (2011).